

## RESEARCH ARTICLE

10.1002/2017JG004080

## Key Points:

- Reducing the temporal resolution of lightning from daily to monthly or yearly decreases simulated burned area in the boreal zone
- The same leads to an increase of burned area in the Tropics and Subtropics
- Excluding the interannual variability of monthly lightning forcing has only a minor effect on simulated burned area

## Correspondence to:

G. Lasslop,  
gitta.lasslop@mpimet.mpg.de

## Citation:

Felsberg, A., Kloster, S., Wilkenskjeld, S., Krause, A., & Lasslop, G. (2018). Lightning forcing in global fire models: The importance of temporal resolution. *Journal of Geophysical Research: Biogeosciences*, 123, 168–177. <https://doi.org/10.1002/2017JG004080>

Received 28 JUL 2017

Accepted 7 DEC 2017

Accepted article online 11 DEC 2017

Published online 23 JAN 2018

## Lightning Forcing in Global Fire Models: The Importance of Temporal Resolution

A. Felsberg<sup>1</sup> , S. Kloster<sup>1</sup>, S. Wilkenskjeld<sup>1</sup>, A. Krause<sup>2</sup>, and G. Lasslop<sup>1</sup>

<sup>1</sup>Land in the Earth System, Max Planck Institute for Meteorology, Hamburg, Germany, <sup>2</sup>Institute for Meteorology and Climate Research, Atmospheric Environmental Research, Karlsruhe Institute of Technology, Garmisch-Partenkirchen, Germany

**Abstract** In global fire models, lightning is typically prescribed from observational data with monthly mean temporal resolution while meteorological forcings, such as precipitation or temperature, are prescribed in a daily resolution. In this study, we investigate the importance of the temporal resolution of the lightning forcing for the simulation of burned area by varying from daily to monthly and annual mean forcing. For this, we utilize the vegetation fire model JSBACH-SPITFIRE to simulate burned area, forced with meteorological and lightning data derived from the general circulation model ECHAM6. On a global scale, differences in burned area caused by lightning forcing applied in coarser temporal resolution stay below 0.55% compared to the use of daily mean forcing. Regionally, however, differences reach up to 100%, depending on the region and season. Monthly averaged lightning forcing as well as the monthly lightning climatology cause differences through an interaction between lightning ignitions and fire prone weather conditions, accounted for by the fire danger index. This interaction leads to decreased burned area in the boreal zone and increased burned area in the Tropics and Subtropics under the coarser temporal resolution. The exclusion of interannual variability, when forced with the lightning climatology, has only a minor impact on the simulated burned area. Annually averaged lightning forcing causes differences as a direct result of the eliminated seasonal characteristics of lightning. Burned area is decreased in summer and increased in winter where fuel is available. Regions with little seasonality, such as the Tropics and Subtropics, experience an increase in burned area.

### 1. Introduction

Besides information on fuel and weather conditions, global fire models require ignition data. Ignitions can be either of anthropogenic or natural origin. Of the natural ignition sources, lightning strokes are most important (Krause et al., 2014; Magi, 2015). Favorable weather conditions can only lead to a fire if an ignition source is present. At the same time, an ignition source can only start a fire if the fire weather conditions, that is, fuel and weather conditions, are suitable. The covariation of fire weather conditions and ignition sources is therefore decisive for fire occurrence.

Representing fire in numerical models remains a challenge, due to the large number of factors influencing fire occurrence and spread as well as additional interdependencies between the factors themselves (Hantson et al., 2016; Lasslop et al., 2014). One difficulty lies in identifying how to best represent lightning strokes leading to ignitions in the model. Current process-based fire models either use a globally constant lightning ignition rate (Hantson et al., 2016; Venevsky et al., 2002) or work with monthly lightning climatologies from observations (Hantson et al., 2016). The latter are either used as such or altered by allocating lightning to days with precipitation, scaling it interannually or interpolating it (Hantson et al., 2016). Daily lightning climatologies are only available with a coarse spatial resolution and are less suitable for global climate simulations. Lightning climatologies are, for example, obtained from the spaceborne optical sensors “Lightning Imaging Sensor and Optical Transient Detector” (LIS/OTD) which detect pulses of illumination above background levels (Cecil et al., 2014). Lightning has also been parameterized in general circulation models (GCMs). In the GCM ECHAM6 (Giorgetta et al., 2013) this is accomplished by using a nonlinear link between the convective cloud top height and the flash frequency (Krause et al., 2014; Price & Rind, 1992), a commonly used parameterization showing higher correlations to observed lightning (LIS/OTD) than other parameterizations

(Clark et al., 2017). As parameterizations of lightning in atmospheric models still show a large magnitude of uncertainty (Magi, 2015) and require rather high computational effort, climatologies are often preferred.

Mean monthly climatologies can reasonably represent the seasonal cycle in global lightning (Magi, 2015). Nevertheless, variations within a month as well as interannual variations are excluded (Clark et al., 2015). The covariation with fire weather conditions, which vary from day to day, is hence not conserved. Further information on the covariation of fire weather conditions and ignition sources is lost by combining observed lightning forcing and, for instance, modeled precipitation. This study investigates to what degree this exclusion of temporal variation of lightning influences the simulation of fire in JSBACH-SPITFIRE. Within the model, variations in fire occurrence are driven by daily variations in fire weather conditions and the number of ignition events (Lasslop et al., 2014; Thonicke et al., 2010).

For this study we compare burned area results from four sensitivity simulations using the global vegetation model JSBACH-SPITFIRE. JSBACH-SPITFIRE is the land component of the GCM ECHAM (Giorgetta et al., 2013), that has been extended by the fire model SPITFIRE (Lasslop et al., 2014). Simulations are forced with daily, monthly and annually averaged lightning flash frequencies and one monthly lightning climatology. The averages as well as the climatology are created from the same 6-hourly lightning data simulated with ECHAM6, the latest version of the GCM ECHAM. The meteorological forcing for JSBACH-SPITFIRE was extracted from the same ECHAM6 simulation to ensure that simulated fire weather and lightning ignitions are consistent.

## 2. Methods

### 2.1. Model

In this study, we use both the atmosphere and the land component of the Earth System Model of the Max Planck Institute for Meteorology (MPI-ESM) (Giorgetta et al., 2013). Fire is simulated in the land surface model JSBACH (Brovkin et al., 2009; Raddatz et al., 2007; Reick et al., 2013) following the process-based fire model SPITFIRE (Thonicke et al., 2010). The implementation of SPITFIRE into JSBACH is described in detail in Lasslop et al. (2014). In the following, we briefly highlight aspects of the model that are relevant for the present study.

The burned fraction BF in one grid box, which is set to  $1.875^\circ \times 1.875^\circ$  in this study, depends on the expected number of ignitions  $E_{n_{ig}}$  per grid box, the mean fire danger index  $FDI$ , and the mean fire area  $\bar{a}_f$  as fraction per grid box.

$$BF = E_{n_{ig}} \cdot FDI \cdot \bar{a}_f \quad (1)$$

The expected number of ignitions  $E_{n_{ig}}$  is defined as the sum of the number of lightning and human ignition events,  $n_{ig_l}$  and  $n_{ig_h}$ , ranging in the magnitude of 0.0001 to 0.001 ignitions per day and  $\text{km}^2$ . The  $n_{ig_l}$  depends on cloud-to-ground lightning flash frequencies, while  $n_{ig_h}$  is prescribed in the model and depends nonlinearly on the population density as well as an assumed, spatially varying propensity of the local population to produce fire.

The fire danger index  $FDI$  describes the probability of an ignition event to result in a fire. It ranges between zero, if the grid cell contains no or only wet fuel, and one, if the fuel is completely dry. For all states in between these two extremes, the  $FDI$  increases with decreasing fuel moisture. An ignition event does not necessarily lead to a fire if ground conditions are not favorable. It is therefore the product of  $E_{n_{ig}}$  and  $FDI$  which can be interpreted as the expected number of fires  $E_{n_f}$ .

The mean fire area  $\bar{a}_f$  indicates a typical area one fire will burn in one grid box according to the prevalent environmental conditions such as wind, fuel type, fuel availability, and fuel conditions, including an estimated fire duration, which nonlinearly depends on the  $FDI$ . In the case of completely dry fuel, that is, the  $FDI$  being 1, and one expected ignition, the mean fire area equals the overall burned area.

For more details on the definition of the mentioned parameters, please see the original documentation of the SPITFIRE-model Thonicke et al. (2010).

Lightning flash frequencies, used to determine the expected number of lightning ignitions, are simulated in the GCM ECHAM6 (Giorgetta et al., 2013). They are calculated following the approach introduced by Price and Rind (1992), which is based on a nonlinear link between the convective cloud top height and the total flash frequency. The cloud-to-ground fraction of the total number of lightnings is then obtained through an empirical approach based on the cold cloud depth (Krause et al., 2014; Price & Rind, 1993).

Not every cloud-to-ground lightning ignites a fire, but only those carrying enough energy. Cloud-to-ground flash frequencies are therefore multiplied with an efficiency factor. The efficiency factor was set to 0.04, following the suggestion of Thonicke et al. (2010) based on observational data accumulated by Latham and Williams (2001).

JSBACH-SPITFIRE simulations for this study are carried out in the off-line mode forced with boundary conditions. The atmospheric forcing data as well as the lightning forcing data are taken from a complete ECHAM6 simulation of the years 1980–2004 (Krause et al., 2014); that is, the applied meteorological forcing is consistent with the applied lightning forcing.

## 2.2. Simulation Setup

We conducted four simulations with JSBACH-SPITFIRE using different kinds of temporal averages of the cloud-to-ground lightning forcing data, while applying the same meteorological forcing. Both the lightning forcing data and the meteorological forcing were extracted from the same ECHAM6 simulation, conducted for the years 1980–2004 with 6-hourly output. As JSBACH-SPITFIRE only requires one forcing value per day, both the meteorological and the lightning forcing data were averaged daily. Simulation *Day* uses daily averages of the cloud-to-ground lightning flash frequency, allowing for day-to-day variations. Simulation *Mon* allocates the monthly average to each day of the corresponding month, and simulation *Year* allocates the annual average to each day of the corresponding year. While the lightning forcing of these three simulations still contains interannual variabilities within the 25 years of the simulation period, simulation *MonClim* uses a monthly climatology generated from the 25 years of lightning forcing data. Similarly to simulation *Mon*, the monthly average value is allocated to each day of the corresponding month. In order to achieve a quasi-equilibrium of the fuel load, spinup simulations were conducted separately for each of the four simulations. All simulations were carried out in a grid resolution of  $1.875^\circ \times 1.875^\circ$ .

## 2.3. Comparison to Observations

To evaluate the simulation results in terms of realistic reproduction of the prominent global patterns of burned area occurrence, we compared simulation results to observational data reported within the Global Fire Emissions Database version 4s (GFEDv4s, Randerson et al., 2012; van der Werf et al., 2017). The data can be obtained from [www.globalfiredata.org](http://www.globalfiredata.org), last accessed 29 March 2017.

We used the normalized mean error (NME) and normalized mean-square error (NMSE) as global benchmarking metrics for burned fraction, having been suggested by Kelley et al. (2013) and applied by Lasslop et al. (2014), to evaluate the spatial distribution. Both NME and NMSE compare modeled values (*mod*) to observed values (*obs*) at each grid box (*i*).

$$\text{NME} = \frac{\sum_i |\text{mod}_i - \text{obs}_i|}{\sum_i |\text{obs}_i - \text{obs}|} \quad (2)$$

$$\text{NMSE} = \frac{\sum_i (\text{mod}_i - \text{obs}_i)^2}{\sum_i (\text{obs}_i - \text{obs})^2} \quad (3)$$

A value of zero indicates perfect agreement between model and observations, while values larger than one indicate that the model performs worse than the observational mean.

## 3. Results

This section first presents results of simulation *Day* and compares it to observations before analyzing its differences toward the sensitivity simulations *Mon*, *MonClim*, and *Year* on a global as well as on a regional scale.

### 3.1. Simulated and Observed Burned Area

Figure 1 shows mean annual burned fractions of simulation *Day* compared to those reported within GFEDv4s. Simulation *Day* is the most realistic of the four sensitivity simulations, as lightning and meteorological forcing have the same temporal resolution. It results in a global annual burned area of 442.45 Mha/yr (averaged over the years 1980–2004) which is within the range of observed values of 480.05 Mha/yr (GFEDv4s averaged over the years 1997–2015) and 348 Mha/yr (GFEDv4 averaged over the years 1997–2011, Giglio et al., 2013). Although Figure 1 displays significant regional differences between simulated and observed burned fraction, general characteristics of the global distribution of burned fraction are reproduced by the model. Largest burned fractions are located in Sub-Saharan Africa, reaching up to about 20% (model), respectively 100%

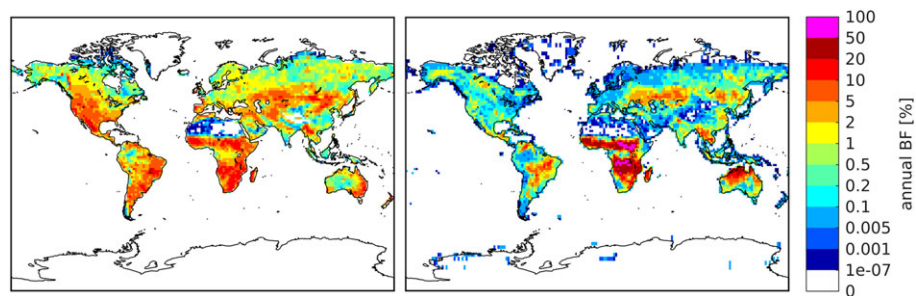


**Figure 1.** Mean annual burned fraction (%). (left) Simulation *Day*, averaged over the years 1980–2004. (right) GFEDv4s, averaged over the years 1997–2015.

(observation). Regions covered by tropical rainforests or deserts exhibit smallest burned fractions, staying below about 2% (model), respectively 0.1% (observation). Moving toward higher latitudes, especially on the Northern Hemisphere, the annual burned fraction decreases to values below about 1% (model), respectively 0.1% (observation). The model underestimates observed values in Sub-Saharan Africa and Australia. In most other regions, the model overestimates observed values (see Figure 1).

Global benchmarking scores take values of 1.02 (NME) and 1.06 (NMSE), the model hence performs worse than the observational mean. Previous studies such as Lasslop et al. (2014) do find much better agreement between JSBACH-SPITFIRE and observations with benchmarking scores of 0.8, respectively 0.87 (NME) and 0.91, respectively 1.0 (NMSE). This is due to the fact that those studies used meteorological forcing from reanalysis such as CRUNCEP and WATCH, while here we use ECHAM6 model output, which, for example, does not reproduce some features of observed precipitation patterns (Hagemann & Stacke, 2015). Using forcing of a GCM often leads to small spatial offsets and therefore strong differences in a grid cell by grid cell comparison. Visual comparison of the patterns shows a reasonable performance of the model, certainly preferable to the observational mean. Improved benchmarking metrics are necessary to better capture the model’s performance in such cases.

**3.2. Sensitivity of Burned Area to the Temporal Resolution of Lightning Forcing**

Differences between the global annual burned area of the sensitivity simulations are very small. Simulation *Day* results in 442.45 Mha/yr, simulation *Mon* in 440.10 Mha/yr, simulation *MonClim* in 440.98 Mha/yr, and simulation *Year* in 440.21 Mha/yr. In comparison to simulation *Day*, values only change by less than 0.55% (see Figure 2, left). Seasonal differences are slightly more pronounced but stay below +1% and –2% for simulations *Mon* and *MonClim*, respectively below +2% and –4% for simulation *Year*.

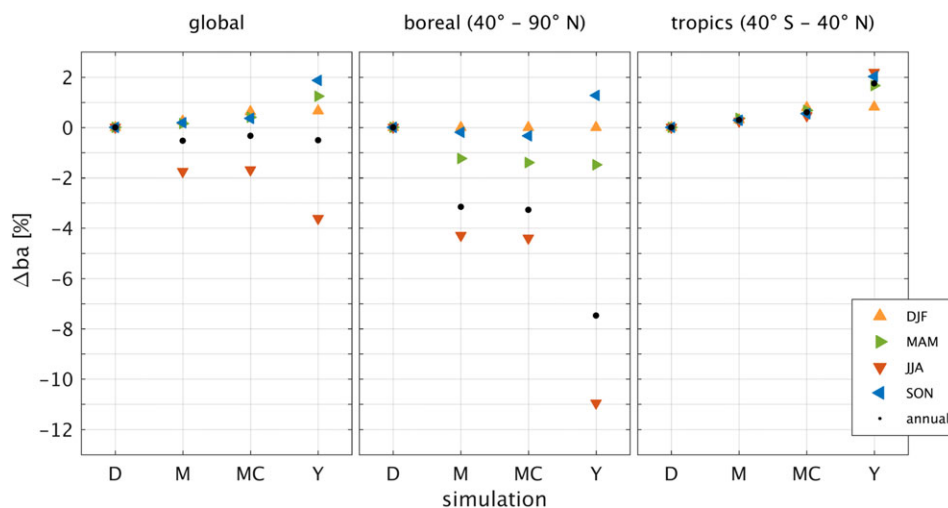


**Figure 2.** Differences of average annual (black) and seasonal (colored) burned area (%) between simulations *Mon* (M), *MonClim* (MC), and *Year* (Y) in reference to simulation *Day* (D). Differences are shown (left) globally, (middle) for the boreal zone (40–90°N), and (right) the Tropics and Subtropics (40°S–40°N).

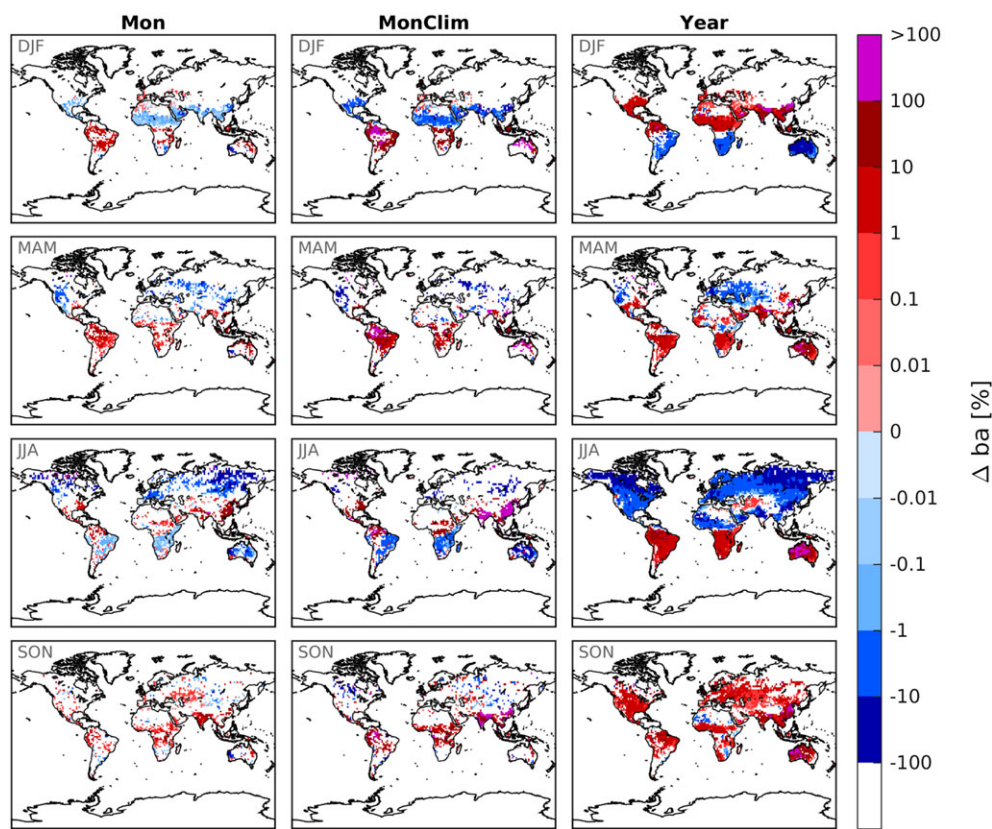


**Figure 3.** Seasonal differences of burned area in reference to simulation *Day* (%). (left column) Simulation *Mon*, (middle column) simulation *MonClim*, (right column) simulation *Year*. From top to bottom, seasons DJF, MAM, JJA, and SON. White: differences do either not exist or are nonsignificant.

Regional differences in comparison to simulation *Day*, however, reach up to about 100%, depending on the region and season (see Figure 3). The distributions of differences in burned area are very similar for simulations *Mon* and *MonClim*. Major negative differences ( $>1\%$ ) are located in the Northern Hemisphere midlatitudes and boreal zone. Here simulations *Mon* and *MonClim* lead to smaller burned area than simulation *Day*. Major positive differences ( $>1\%$ ) are located in the Tropics and Subtropics. Here simulations *Mon* and *MonClim* lead to larger burned area than simulation *Day*. The differences are most pronounced for the seasons March–April–May (MAM) and June–July–August (JJA) (see Figure 3).

Between *Mon* and *MonClim*, small differences in simulated burned area do exist (mostly  $< \pm 1\%$ , not shown). The burned area is slightly larger in the boreal zone for simulation *Mon* in comparison to simulation *MonClim* (by about 0.1% to 1%, see Figure 2). In the Subtropics and Tropics simulation *Mon* leads to a larger burned area for the winter hemispheres (Northern Hemisphere during December–January–February (DJF), by about 0.1%, and Southern Hemisphere during JJA, by about 0.1% to 10%), while simulation *MonClim* leads to slightly larger burned area for the summer hemispheres (Northern Hemisphere during JJA, by about 0.1% to 10%, and Southern Hemisphere during DJF, by up to 1%). During MAM and September–October–November (SON), burned area in the Subtropics and Tropics is slightly larger for simulation *MonClim* (by up to 1%).

Simulation *Year* exhibits a different pattern of differences in burned area than simulations *Mon* and *MonClim* (see Figure 3). During DJF, negative differences in burned area are mainly located in the Southern Hemisphere, while they are mostly located in the Northern Hemisphere during JJA (and MAM). Here simulation *Year* leads to smaller burned area than simulation *Day* (by about 1% to 10%). Positive differences are mainly found in the Northern Hemisphere Tropics and Subtropics during DJF (about 1% to 10%) and in the Southern Hemisphere during MAM and JJA (about 1% to 100%). During SON, positive differences dominate globally (mostly less than 1%).

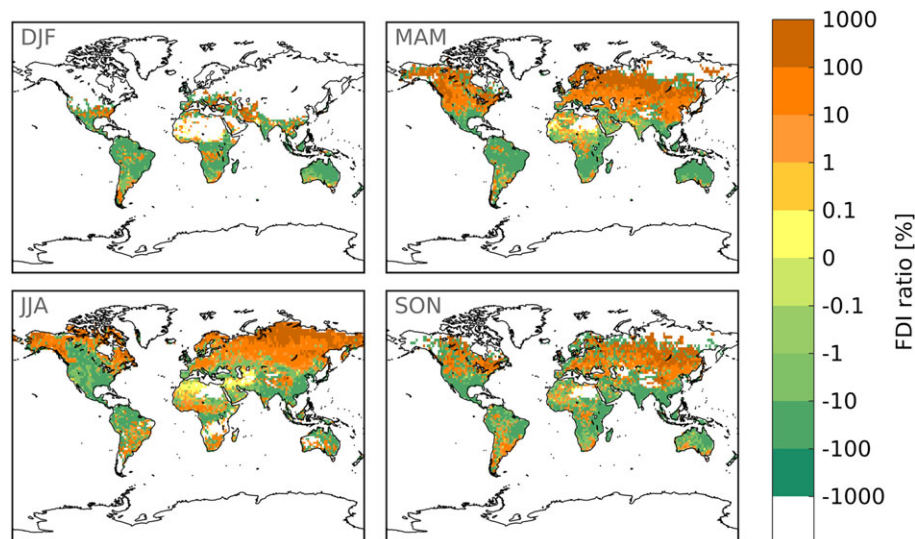


**Figure 4.** Differences between mean fire danger index on days that exhibit lightning ignition and the mean fire danger index of the whole month, within the simulation *Day* (%). Differences are given in reference to the mean fire danger index of the whole month and averaged for each season. White: differences are either zero or a missing value.

Overall, lightning forcing of reduced temporal resolution tends to decrease the simulated burned area in comparison to simulation *Day* for the boreal zone (see Figure 2). For large parts of the Tropics and Subtropics, on the other hand, forcing of broader temporal resolution mostly increases the simulated burned area. Differences for the boreal zone are dominated by conditions in JJA. Here differences in the annual burned area of the boreal zone for simulations *Mon* and *MonClim* reach more than  $-4\%$  and about  $-11\%$  for simulation *Year* (see Figure 2, middle). In the Tropics, the burned area slightly increases with increasing averaging time of the lightning forcing for all seasons. Differences stay below  $+1\%$  for simulations *Mon* and *MonClim* and below  $+2\%$  for simulation *Year* (see Figure 2, right).

#### 4. Discussion

The individual sensitivity simulations only differ in terms of the applied lightning forcing. Lightning frequencies directly impact the number of lightning ignitions. Changes in the number of lightning ignitions will subsequently change the burned area (see equation (1)). Changes in burned area will in turn affect the amount of available fuel. An increase in burned area will, for example, lead to a decrease in available fuel. This change in available fuel modifies the fire danger index *FDI* and the mean fire area  $\bar{a}_f$ , both parameters again directly control the burned area (see equation (1)). Individual changes in *FDI* and  $\bar{a}_f$  within the sensitivity simulations are, however, too small to explain the observed changes in simulated burned area (mostly below  $\pm 1\%$ , not shown). They will hence not be further discussed.

In the boreal zone, lightning occurs much less frequently compared to the Tropics (LIS/OTD, Cecil et al. (2014)). As a consequence, the number of lightning ignitions is high for a small number of days per year in simulation *Day* and zero on all other days. In simulation *Mon*, lightning takes place every day, but the number of lightning ignitions is smaller due to the averaging process. Figure 4 shows that, for the boreal zone, days with lightning ignition in simulation *Day* experience above average *FDI*; that is, the average *FDI* on those days of a month experiencing lightning ignitions is larger than the overall monthly average *FDI* of the same month. Consequently, high numbers of lightning ignitions coincide with a high *FDI*, leading to a large burned area for simulation *Day*. As the number of lightning ignitions is smaller for these days within simulation *Mon* and the *FDI* is on average smaller for the other days of the month, simulated burned area is smaller for simulation *Mon* (by about 3%, see Figure 2). The simultaneous behavior of the number of lightning ignitions and the *FDI* is also discernable in the product of the two (see Figure 5), which by definition is proportional to the burned area (see equation (1)). Figure 5 shows that this product is indeed larger for simulation *Day* in the boreal zone.

In large parts of the Tropics and Subtropics, lightning occurs more often. Accordingly, averaging the lightning over a month as in simulation *Mon* does not significantly reduce the number of lightning ignitions per day.

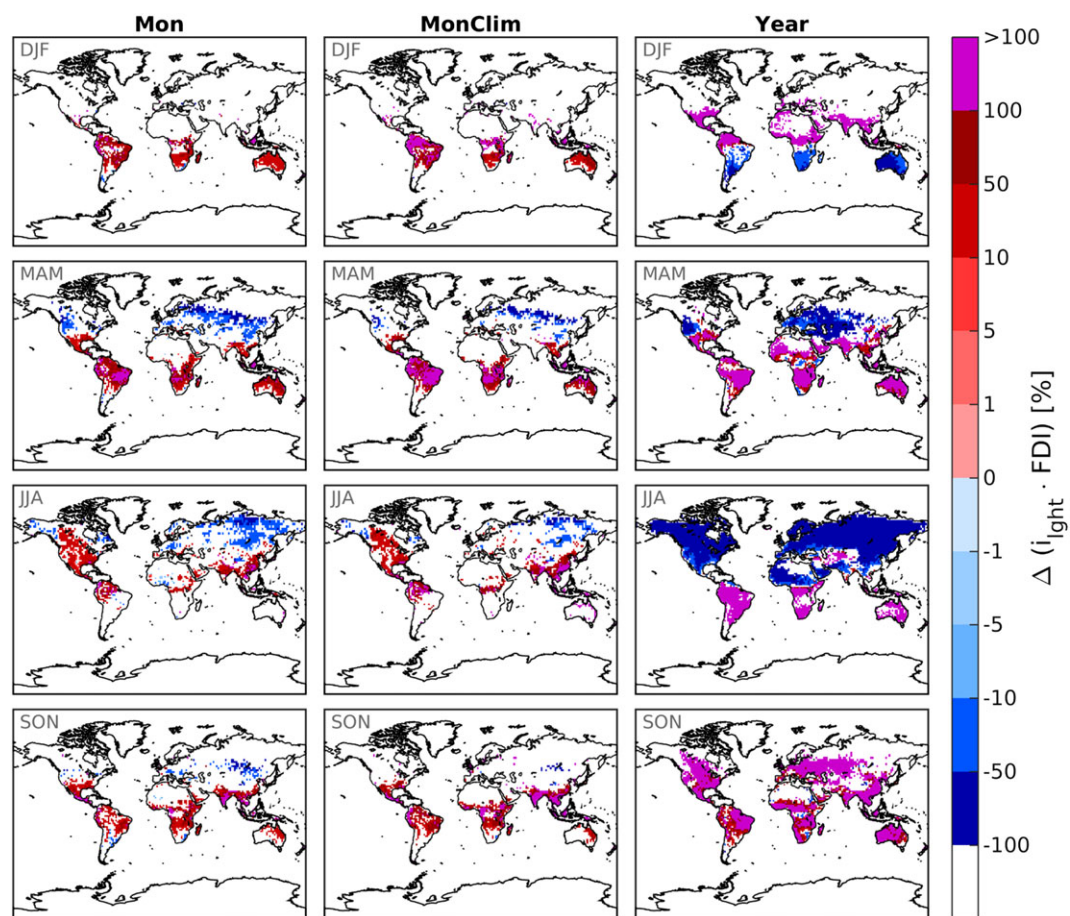


**Figure 5.** Seasonal differences of the product of lightning ignition and fire danger index in reference to simulation *Day* (%). (left) Simulation *Mon*, (middle) simulation *MonClim*, (right) simulation *Year*. From top to bottom, seasons DJF, MAM, JJA, and SON. White: differences do either not exist or are nonsignificant.

Figure 4 shows that days with lightning ignitions taking place in simulation *Day* experience a below average FDI in the Tropics and Subtropics. Consequently, the resulting burned area is smaller (by about 0.5%, see Figure 2). This is underlined by the product of the number of lightning ignitions and the FDI, which is larger for simulation *Mon* in the Tropics and Subtropics (see Figure 5).

We find that, globally, the convective precipitation is above the monthly average on days with lightning ignition and thus cannot explain the different behavior of the fire danger index in the boreal zone and the Tropics for simulations *Day* and *Mon*. We conclude that the different behavior is caused by different vegetation types for which the fuel moisture content reacts differently to precipitation events. In the model, this is accounted for by different drying parameters for the three fuel classes (1 h, 10 h, and 100 h fuels) used to calculate the fire danger index.

Burned area results of simulations *Mon* and *MonClim* are very similar and can be explained by the same processes and interactions as described above (see Figure 5). On top of excluding day to day variations of lightning, the use of a climatology additionally excludes any interannual variability. As sporadic extreme events are important for the simulation of large burned area in the boreal zone, the use of monthly lightning climatologies instead of monthly averages decreases the boreal burned area even further (by about 1%, see Figure 2).

Monthly averaging of the lightning forcing only excludes variations within a month while retaining seasonal characteristics. Annual averaging of the lightning forcing, as in simulation *Year*, however, also excludes these month to month variations. Regions with strong lightning seasonality, such as the mid northern latitudes, the boreal zone and the Southern Hemisphere Subtropics, are therefore strongly affected (by up to about 10%, see Figure 3). Here lightning frequencies and subsequently the number of lightning ignitions,

are decreased during summer and increased during winter. In summer, similar to simulation *Mon*, simulation *Year* therefore shows strongly decreased burned area in comparison to simulation *Day* (in sum by about 11%, see Figure 2). Differences are, however, much more pronounced than for simulations *Mon* and *MonClim* as lightning frequencies and subsequently their product with the *FDI* are also much lower (see Figure 5). In winter, the increased number of lightning ignitions causes an increase in burned area in the Southern Hemisphere Subtropics (by up to about 10%). In the mid northern latitudes and the boreal zone, on the other hand, this is inhibited by the presence of snow, the absence of fuel, or its moisture content. The burned area deficit from Northern Hemisphere summer therefore cannot be compensated, so that the overall annual burned area in the boreal zone is decreased for simulation *Year* (by about 7%, see Figure 2).

In regions with less lightning seasonality, such as the Tropics and Subtropics, differences in burned area are mainly positive; that is, simulation *Year* results in larger burned area than simulation *Day* (by about 2%, see Figure 3). Similar to simulation *Mon*, the averaging process prevents a limitation of fire occurrence through low *FDI*, as is the case on days with lightning ignition within simulation *Day* (see Figure 4). The product of *FDI* and the number of lightning ignitions is hence larger for simulation *Year* than for simulation *Day* (see Figure 5).

As for simulations *Mon* and *MonClim*, differences of the product of *FDI* and the number of lightning ignitions in comparison to simulation *Day* fit well to the distribution of differences in burned area (see Figure 5). For simulation *Year*, however, this product is strongly dominated through differences in the number of lightning ignitions (not shown). Since these are more pronounced due to the longer averaging time period, it is only natural that their effect on simulated burned area is also increased.

## 5. Conclusion

In this study, we analyzed the impact of temporal variations of lightning on the simulation of burned area within JSBACH-SPITFIRE. We compared four sensitivity simulations that were forced with daily, monthly, and yearly averages of lightning flash frequency as well as a lightning climatology while all other forcing data were identical.

On a global scale, burned area results did not exhibit large differences between the four sensitivity simulations (<0.55%). On a regional scale, differences in burned area become drastically more important (up to about 100% in northern Canada, Siberia, Australia, and the Amazon). An interaction between fire prone weather conditions, accounted for by the fire danger index, and elevated lightning activity is responsible for most observed differences larger than  $\pm 1\%$ .

Compared to simulation *Mon*, simulation *Day* leads to larger burned area in the middle and high latitudes of the Northern Hemisphere. This is in good accordance with general characteristics of the fire regime in this region. Fires in boreal forests are of low frequency and aperiodic, because conditions are rarely sufficiently dry (Bistinas et al., 2014; Kasischke et al., 2002). Here most of the total burned area results from only a few large fires as they can last for several weeks or months (Pfeiffer et al., 2013; Stocks et al., 2002). For these low-frequency fires in the boreal zone, lightning is the dominant ignition source (Pfeiffer et al., 2013; Stocks et al., 2002; Veraverbeke et al., 2017). A monthly average of the lightning forcing reduces the number of lightning ignitions on days with high fire danger indices and consequently reduces the simulated burned area. A realistic simulation of fires in the boreal zone might be of importance not only for burned area results but also for the simulation of fire emissions. Clark et al. (2015) conclude that, especially in high latitudes, fire emissions are better represented by short but intense emission pulses instead of a steady emission. This is only possible if infrequent large fires are simulated instead of frequent small fires.

Simulation *Mon*, on the other hand, leads to larger burned area in the Tropics and Subtropics throughout the year when compared to simulation *Day*. Tropical savanna and grassland fires occur more regularly and frequent and are thus less episodic than fires in the boreal zone. Average lightning flash frequencies for these regions are, in general, higher than for the boreal zone. Still, fire occurrence is limited by below average fire danger indices on days of lightning occurrence. A forcing of monthly averaged lightning flash frequencies ensures that days with high fire danger indices encounter lightning ignitions. The burned area is therefore increased by the use of monthly mean lightning forcing. Please note, however, that particularly in the Tropics and Subtropics most fires are the result of deliberate human fire management (Galanter et al., 2000). Lightning ignitions and the impact of the temporal resolution of the lightning forcing might only be of secondary importance for realistic fire simulations in these regions.

These conclusions and principles are also valid for simulation *MonClim*. Its main effect on the burned area is caused by the monthly averaging of lightning frequencies in the course of creating a monthly climatology. The removal of interannual variability does slightly alter the amount of simulated burned area when compared to simulation *Mon*, but differences mostly stay below  $\pm 1\%$  with the exceptions of some extreme values. Although the overall impact is hence small, some regions, such as northern North America, might still be strongly impacted by the removal of interannual variation of lightning. For this region, Veraverbeke et al. (2017) found that 36% to 43% of the interannual variation in burned area can be attributed to lightning ignitions alone.

In simulation *Year*, simulated burned area is strongly affected in regions with strong lightning seasonality, such as the mid northern latitudes, the boreal zone, and the Southern Hemisphere Subtropics. Here annual averaging of the lightning frequency eliminates any seasonal characteristic, thereby decreasing burned area in summer and increasing it in winter if possible. In regions with weaker lightning seasonality, simulation *Year* results in larger burned area than simulation *Day* due to the redistribution of lightning ignitions throughout the year.

To contextualize the magnitude of found differences in burned area, we tested the extremes of the lightning forcing being globally zero as well as applying the value of the grid box with maximum annual lightning frequency (of 4.30 flashes/s). Annual global burned area was 427.22 Mha/yr for the first case and 526.39 Mha/yr for the second case. Maximum differences in annual burned area compared to simulation *Day* are hence limited to a range between  $-3.44\%$  and about  $18.97\%$ , emphasizing the importance of the covariation with fuel and weather conditions for large burned area to occur.

The general conclusion of this study, that a change of the temporal resolution of the employed lightning forcing leads to changes in simulated burned area, can be assumed universally valid. Interactions between lightning and fire danger seasonality should be similar for JSBACH-SPITFIRE and other fire models. When investigating extreme events or focusing on boreal regions, we therefore recommend the use of daily lightning forcing if possible and emphasize that climatologies might lead to inaccuracies due to the exclusion of extreme lightning events. For an analysis of global burned area, it might, on the other hand, be worth to save computational time and use averaged values (monthly, annually, or climatologies) as differences in global annual burned area are minor. Nevertheless, the way in which models account for fire ignitions varies (Hantson et al., 2016), so that the presented results have to be quantified individually.

#### Acknowledgments

We acknowledge the DKRZ for providing excellent computing facilities. Primary data and scripts used in the analysis and other supplementary information that may be useful in reproducing the author's work are archived by the Max Planck Institute for Meteorology and can be obtained by contacting publications@mpimet.mpg.de or under [https://cera-www.dkrz.de/WDC/ui/Entry.jsp?acronym=DKRZ\\_lta\\_060\\_1](https://cera-www.dkrz.de/WDC/ui/Entry.jsp?acronym=DKRZ_lta_060_1).

#### References

- Bistinias, I., Harrison, S., Prentice, I., & Pereira, J. (2014). Causal relationships vs. emergent patterns in the global controls of fire frequency. *Biogeosciences Discussions*, *11*(3), 3865–3892.
- Brovkin, V., Raddatz, T., Reick, C. H., Claussen, M., & Gayler, V. (2009). Global biogeophysical interactions between forest and climate. *Geophysical Research Letters*, *36*, L07405. <https://doi.org/10.1029/2009GL037543>
- Cecil, D. J., Buechler, D. E., & Blakeslee, R. J. (2014). Gridded lightning climatology from TRMM-LIS and OTD: Dataset description. *Atmospheric Research*, *135*, 404–414.
- Clark, S. K., Ward, D. S., & Mahowald, N. M. (2015). The sensitivity of global climate to the episodicity of fire aerosol emissions. *Journal of Geophysical Research: Atmospheres*, *120*, 11,589–11,607. <https://doi.org/10.1002/2015JD024068>
- Clark, S. K., Ward, D. S., & Mahowald, N. M. (2017). Parameterization-based uncertainty in future lightning flash density. *Geophysical Research Letters*, *44*, 2893–2901. <https://doi.org/10.1002/2017GL073017>
- Galanter, M., Levy, H., & Carmichael, G. R. (2000). Impacts of biomass burning on tropospheric CO, NO<sub>x</sub>, and O<sub>3</sub>. *Journal of Geophysical Research*, *105*(D5), 6633–6653.
- Giglio, L., Randerson, J. T., & van der Werf, G. R. (2013). Analysis of daily, monthly, and annual burned area using the fourth-generation Global Fire Emissions Database (GFED4). *Journal of Geophysical Research: Biogeosciences*, *118*, 317–328. <https://doi.org/10.1002/jgrg.20042>
- Giorgetta, M. A., Jungclaus, J., Reick, C. H., Legutke, S., Bader, J., Böttinger, M., ... Stevens, B. (2013). Climate and carbon cycle changes from 1850 to 2100 in MPI-ESM simulations for the Coupled Model Intercomparison Project phase 5. *Journal of Advances in Modeling Earth Systems*, *5*(3), 572–597.
- Hagemann, S., & Stacke, T. (2015). Impact of the soil hydrology scheme on simulated soil moisture memory. *Climate Dynamics*, *44*(7–8), 1731–1750.
- Hantson, S., Arneth, A., Harrison, S. P., Kelley, D. I., Prentice, I. C., Rabin, S. S., ... Yue, C. (2016). The status and challenge of global fire modelling. *Biogeosciences*, *13*(11), 3359–3375.
- Kasischke, E. S., Williams, D., & Barry, D. (2002). Analysis of the patterns of large fires in the boreal forest region of Alaska. *International Journal of Wildland Fire*, *11*(2), 131–144.
- Kelley, D., Prentice, I. C., Harrison, S., Wang, H., Simard, M., Fisher, J., & Willis, K. (2013). A comprehensive benchmarking system for evaluating global vegetation models. *Biogeosciences*, *10*(5), 3313–3340.
- Krause, A., Kloster, S., Wilkenskjeld, S., & Paeth, H. (2014). The sensitivity of global wildfires to simulated past, present, and future lightning frequency. *Journal of Geophysical Research: Biogeosciences*, *119*, 312–322. <https://doi.org/10.1002/2013JG002502>
- Lasslop, G., Thonicke, K., & Kloster, S. (2014). SPITFIRE within the MPI Earth system model: Model development and evaluation. *Journal of Advances in Modeling Earth Systems*, *6*(3), 740–755.

- Latham, D., & Williams, E. (2001). Lightning and forest fires. In E. A. Johnson & K. Miyanishi (Eds.), *Forest fires: Behavior and ecological effects* (pp. 375–418). New York: Academic Press.
- Magi, B. I. (2015). Global lightning parameterization from CMIP5 climate model output. *Journal of Atmospheric and Oceanic Technology*, 32(3), 434–452.
- Pfeiffer, M., Spessa, A., & Kaplan, J. (2013). LPJ-LMfire: An improved fire module for dynamic global vegetation models. *Geoscientific Model Development Discussions*, 6, 643–685.
- Price, C., & Rind, D. (1992). A simple lightning parameterization for calculating global lightning distributions. *Journal of Geophysical Research*, 97(D9), 9919–9933.
- Price, C., & Rind, D. (1993). What determines the cloud-to-ground lightning fraction in thunderstorms? *Geophysical Research Letters*, 20(6), 463–466.
- Raddatz, T., Reick, C., Knorr, W., Kattge, J., Roeckner, E., Schnur, R., ... Jungclaus, J. (2007). Will the tropical land biosphere dominate the climate–carbon cycle feedback during the twenty-first century? *Climate Dynamics*, 29(6), 565–574.
- Randerson, J., Chen, Y., Werf, G., Rogers, B., & Morton, D. (2012). Global burned area and biomass burning emissions from small fires. *Journal of Geophysical Research*, 117, G04012. <https://doi.org/10.1029/2012JG002128>
- Reick, C., Raddatz, T., Brovkin, V., & Gayler, V. (2013). Representation of natural and anthropogenic land cover change in MPI-ESM. *Journal of Advances in Modeling Earth Systems*, 5(3), 459–482.
- Stocks, B. J., Mason, J. A., Todd, J. B., Bosch, E. M., Wotton, B. M., Amiro, B. D., ... Skinner, W. R. (2002). Large forest fires in Canada, 1959–1997. *Journal of Geophysical Research*, 107(D1), 8149. <https://doi.org/10.1029/2001JD000484>
- Thonicke, K., Spessa, A., Prentice, I., Harrison, S. P., Dong, L., & Carmona-Moreno, C. (2010). The influence of vegetation, fire spread and fire behaviour on biomass burning and trace gas emissions: Results from a process-based model. *Biogeosciences*, 7(6), 1991–2011.
- van der Werf, G. R., Randerson, J. T., Giglio, L., van Leeuwen, T. T., Chen, Y., Rogers, B. M., ... Kasibhatla, P. S. (2017). Global fire emissions estimates during 1997–2016. *Earth System Science Data*, 9, 697–720.
- Venevsky, S., Thonicke, K., Sitch, S., & Cramer, W. (2002). Simulating fire regimes in human-dominated ecosystems: Iberian Peninsula case study. *Global Change Biology*, 8(10), 984–998.
- Veraverbeke, S., Rogers, B. M., Goulden, M. L., Jandt, R. R., Miller, C. E., Wiggins, E. B., & Randerson, J. T. (2017). Lightning as a major driver of recent large fire years in North American boreal forests. *Nature Climate Change*, 7(7), 529–534.